pubs.acs.org/Biomac

Article

Catalytic Detoxification of Organophosphorus Nerve Agents by Butyrylcholinesterase-Polymer-Oxime Bioscavengers

Libin Zhang, Hironobu Murata, Gabriel Amitai, Paige N. Smith, Krzysztof Matyjaszewski, and Alan J. Russell*

Cite This: *Biomacromolecules* 2020, 21, 3867−3877

Read Online

ACCESS | Metrics & More | Article Recommendations | Supporting Information

ABSTRACT: Organophosphorus nerve agents (OPNAs), used in chemical warfare, irreversibly inhibit essential cholinesterases (ChEs) in the cholinergic neurotransmission system. Several potent nucleophilic oximes have been approved for the treatment of acute poisoning by OPNAs, but they are rapidly cleared from blood circulation. Butyrylcholinesterase (BChE) stoichiometrically binds nerve agents, but because the molecular weight of a nerve agent is about 500-fold less than the enzyme, the bioscavenger has had limited utility. We synthesized BChE-polymer-oxime conjugates using atom transfer radical polymerization (ATRP) and azide−alkyne "click" chemistry. The activity of the BChE-polymer-oxime conjugates was dependent on the degree of oxime loading within the copolymer side chains. The covalent modification of oxime-containing copolymers prolonged the activity of BChE in the presence of the VX- and cyclosarin-fluorogenic analogues EMP-MeCyC and CMP-MeCyC, respectively. After complete inactivation by VX and cyclosarin fluorogenic analogues, the conjugates demonstrated efficient self-reactivation of up to 80% within 3−6 h. Repeated inhibition and high-level self-reactivation assays revealed that the BChE-polymer-oxime conjugates were excellent reactivators of OPNA-inhibited BChE. Recurring self-reactivation of BChE-polymer-oxime conjugates following repeated BChE inhibition by fluorogenic OPNAs (Flu-OPNAs) opens the door to developing the next generation of nerve agent "catalytic" bioscavengers.

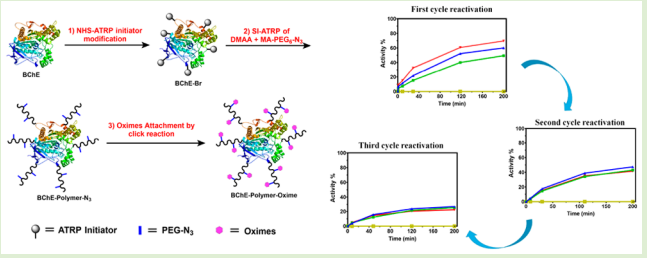

INTRODUCTION

Initially developed in the 1930s, organophosphorus nerve agents (OPNAs) have been used as pesticides, tested on criminal subjects, used in terrorist acts, and employed as chemical warfare agents.[1] Tabun and sarin, for example, were used in the Iran−Iraq war in the 1980s; sarin was used against civilians in Syria and by a terrorist sect in the Tokyo subway, and VX was used to assassinate the North Korean, Kim Jong-nam, in Malaysia (2017).[2−5] Accidental and self-poisoning by organophosphorus pesticides results in around 100 000 deaths and affects more than 1 million people each year worldwide.[6] OPNAs inhibit cholinesterases (ChEs) in the cholinergic neurotransmission system[7] by phosphorylation of a catalytic serine residue in the active site. OPNA toxicity results from the accumulation of neurotransmitters in cholinergic synapses leading to paralysis, hypotension, breathing failure, and death.[8−11] Hydrophobic OPNAs cross the blood−brain barrier (BBB) and inactivate acetylcholinesterase (AChE) in the central nervous system (CNS). Accumulated OPNAs, retained in the CNS, can also partition back into blood, causing "cholinergic crisis" and irreversible brain damage.[12,13]

Currently approved treatment of acute OPNA poisoning includes administration of a mixture of a pyridinium aldoxime, an anticonvulsant (benzodiazepine), and a muscarinic acetylcholine receptor antagonist (atropine).[14,15] Since the seminal work of Wilson and colleagues in the mid-1950s, thousands of aldoximes have been synthesized and screened.[16,17] A few molecules, for example pralidoxime (2-PAM), asoxime (HI-6), and obidoxime (toxogonin), have been developed as OPNA poisoning therapeutics.[14,15] Aldoximes, in the charged oximate nucleophilic state, attack the phosphoryl bond of covalently inhibited ChEs at the active site serine, releasing the OP moiety from the active site and restoring ChE activity.[18−20] Over several decades, numerous imidazolium oximes have been developed as OP-ChE reactivators.[12,21−24] Some of these derivatives were shown to be efficient reactivators in specific *in vitro* and *in vivo* reactivation assays using VX- and tabun-inhibited ChEs.[23−27] Antidotal therapy by oximes, unfortunately, requires repeated administration because low molecular weight oximes have very

Received: June 22, 2020
Revised: July 26, 2020
Published: July 31, 2020

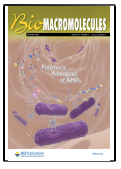

https://dx.doi.org/10.1021/acs.biomac.0c00959
Biomacromolecules 2020, 21, 3867−3877

short half-lives in circulation.[28,29] This short half-life also limits the use of oximes as effective long-term prophylactic drugs.

A new concept of acute OPNA poisoning treatment, by the administration of bioscavengers, emerged at the end of the 1980s.[30−35] Bioscavengers are proteins that react with and neutralize OPNAs. Human butyrylcholinesterase (BChE) is effective as a bioscavenger at both pre- and post-OPNA exposure.[36−40] The enzyme is stable in human blood circulation, with a half-life of 12 days, in concentration ranges between 3.5 and 9.3 mg/L.[41−45] BChE is found in plasma, organs, and tissues including liver, skin, striated muscle, smooth muscle, lung, and brain.[46] Administration of BChE has proven to be safe with no toxic, immunogenic, or behavioral effects.[47] As a stoichiometric bioscavenger with a molecular weight of about 85 kDa, 500−600 times higher than that of OPNAs, a relatively high dose of BChE (100−500 mg) is required to effectively protect a 70 kg patient.[48] Unfortunately, this dose costs more than $2000, and therefore, BChE therapy has not been deployed as a prophylactic drug.[30]

Grafting poly(ethylene glycol) (PEG)[49−52] and poly(sialic acid) to the surface of BChE has been used to increase the half-life of the enzyme in the blood.[53−56] Nevertheless, even extended lifetime BChE does not overcome the inherent limitations of a stoichiometric bioscavenger. We have become interested in whether polymers could serve to increase BChE protein lifetime while also enabling reactivation and protection of the enzyme, thereby defeating the stoichiometric limitations that drive up the necessary dose. Such a self-reactivating BChE protein−polymer conjugate could also be used as a critical component in decontamination of broad areas.

A "grafting from" high yield approach to protein−polymer conjugate synthesis, involving the *in situ* growth of polymers from biomacromolecular initiators, emerged in the early 2000s.[57−59] Developed in the early 1990s, atom transfer radical polymerization (ATRP) has proved to be a controlled and powerful technique to prepare well-defined polymers and protein−polymer conjugates.[51,60−65] With a long-term interest in polymer-based protein engineering, we have generated a large library of protein−polymer conjugates.[66−69]

In the past decade, first generation "pseudo-catalytic" bioscavenger systems composed of BChE delivered with an efficient oxime reactivator were developed to reduce the amount of BChE needed for efficient protection.[23,24,36,70] Unfortunately, the fast elimination of oxime reactivators from blood circulation, requiring continuous infusion of the reactivator to sustain reactivation kinetics, limited the use of pseudo-catalytic bioscavengers *in vivo*.[30] Most recently, we have used ATRP to synthesize BChE-polymer conjugates with multiple pendant azido groups. Azide−alkyne "click" chemistry was then used to covalently couple oximes to the surface of the enzyme.[71] The BChE-polymer-oximes exhibited a slowed rate of inactivation by organophosphates and some evidence of inter- and intramolecular reactivation. Herein, fluorogenic analogues of VX and cyclosarin (EMP-MeCyC and CMP-MeCyC, respectively)[72] were used to study the kinetics of inactivation and reactivation of next-generation BChE-polymer-oxime conjugates. The BChE-polymer-oxime conjugate recovered about 85% activity after complete inactivation induced by fluorogenic analogues of VX in three successive inactivation−reactivation "catalytic" cycles. The conjugates should also be useful in surface decontamination of OPNAs.

EXPERIMENTAL SECTION

Materials. Common reagents and solvents were purchased from Fisher Scientific (Pittsburgh, PA) and used as received unless otherwise specified. Dr. Oksana Lockridge (Eppley Institute, University of Nebraska Medical Center) kindly provided the human BChE. EMP-MeCyC and CMP-MeCyC were prepared as described previously.[72] MA-PEG$_6$-N$_3$ monomer and NHS-Br (ATRP initiator) were prepared in the same way as our previous reports.[71,73] Copper(II) bromide ($CuBr_2$), copper(II) sulfate ($CuSO_4$), hydroxylamine hydrochloride, triethylamine, sodium ascorbate (NaAsc), 2-imidazolecarboxaldehyde, *S*-butyrylthiocholine iodide (BTC), 5,5′-dithiobis (2-nitrobenzoic acid) (DTNB), *N*,*N*-dimethylacrylamide (DMAA), 1,1,4,7,10,10-hexamethyltriethylenetetramine (HMTETA), tris[2-(dimethylamino)ethyl] amine (Me$_6$TREN), isonicotinaldehyde, 1,4-diiodobutane, 6-iodohex-1-yne, and 4-chlorobenzyl bromide were purchased from Sigma-Aldrich. DMAA, Me$_6$TREN, and HMTETA were purified with a basic alumina column before use. 2-(4-((Bis((1-(*tert*-butyl)-1*H*-1,2,3-triazol-4-yl)methyl)amino)methyl)-1*H*-1,2,3-triazol-1-yl) acetic acid (BTTAA) and azide-PEG-amine were purchased from Click Chemistry Tools LLC. *N*,*N*-Dimethylprop-2-yn-1-amine was purchased from Fisher Scientific.

Characterization. *Nuclear Magnetic Resonance (NMR) Analysis.* A 400 MHz spectrometer (Bruker Avance) in the Center for Molecular Analysis, Carnegie Mellon University, Pittsburgh, PA was used to collect ^{1}H NMR spectra.

Ultraviolet−Visible (UV−vis) and Fluorescence Spectrophotometry. UV−vis spectra were analyzed by a UV−VIS spectrophotometer (Lambda 45, PerkinElmer). Fluorescence spectra were analyzed by a plate reader (Bio-Tek Synergy H1).

GPC Analysis. The molecular weight (M_n) and the polydispersity ($Đ$) of azide containing copolymers were determined by GPC with 3-columns on a Waters 2695 Series system (Waters Ultrahydrogel Linear, 500 and 250) as in our previous report.[71] The BChE, BChE-Br, BChE-PDMAA-N$_3$, and BChE-PDMAA-OX conjugates were analyzed by the same GPC system with four columns.

Protein Analysis by the Bicinchoninic Acid (BCA) Assay. The BChE-PDMAA-OX conjugate (1−2 mg/mL, protein, 20 or10 μL) in BP buffer (50 mM, pH 7.4) was mixed with 200 μL of BCA working reagent solution (Reagent A/Reagent B = 50/1). The mixture was incubated at 60 °C for 15 min. Absorbance of the samples at 562 nm was recorded by a plate reader (Bio-Tek Synergy H1). Standard curves of PEG-IO, PEG-PO, and native BChE were used to determine the protein concentration of the conjugates (Figure S1).

SDS-PAGE Analysis. BChE, BChE-Br, or BChE-polymer-oxime conjugate solution (1.0 mg/mL protein, 10 μL) was mixed with SDS-PAGE loading buffer (2×, 10 μL) and heated at 95 °C for 10 min. Ten microliters of the sample was loaded onto 4−15% precast gel and run at 200 V for 30 min. The gel was washed with distilled water three times and stained with 50 mL of PageBlue staining solution. One hour later, the gel was destained overnight using distilled water.

Methods. *Synthesis of Alkyne-Imidazolium-Oxime.* Alkyne-imidazolium-oxime was synthesized as described previously.[71] Briefly, 2-imidazolecarboxaldehyde (12 mmol) and K_2CO_3 (24 mmol) were mixed in 30 mL of DMF. 4-Chlorobenzyl bromide (24 mmol) was added and stirred at room temperature overnight. The reaction mixture was filtered, and 250 mL of distilled water was added to the filtrate. The resulting solution was extracted with ethyl acetate (200 mL × 3); then, the organic phase was dried with $MgSO_4$. After the solvent was removed using a rotary evaporator, the alkylimidazole-2-carbaldehyde yield was 74%.

Hydroxylamine hydrochloride (13.5 mmol) was dissolved in 30 mL of water and added to Na_2CO_3 (13.5 mmol) and alkylimidazole-2-carbaldehyde (9 mmol). The reaction mixture was stirred for 3.5 h at room temperature, and the precipitate was filtered and washed using distilled water three times and Et_2O four times. The product was dried over a vacuum, generating an 87% yield.

6-Iodohex-1-yne (1.5 mmol) in 10 mL of ACN and 1 mL of DMSO was added to the alkylimidazole-2-carbaldehyde oxime (0.4 mmol). The reaction mixture was stirred at 67 °C for 5 days. The solvent was removed by rotary evaporator. The crude product was

https://dx.doi.org/10.1021/acs.biomac.0c00959
Biomacromolecules 2020, 21, 3867−3877

purified by silica gel column (from hexane/acetone = 1/1 to acetone/MeOH = 3/1). White powder, 48% yield. ^{1}H NMR (400 MHz, MeOD-d4) δ 8.52 (s, 1H, CH), 7.82 (d, J = 3, 1H, Ar H), 7.74 (d, J = 3, 1H, Ar H), 7.44 (d, J = 3, 2H, Ar H), 7.35 (d, J = 3, 2H, Ar H), 5.63 (s, 2H; CH_2), 4.43 (t, J = 3, 2H; CH_2), 3.36 (s, 1H; CH), 2.27 (d, J = 3, 2H, CH_2), 2.02−2.00 (m, 2H; CH_2), 1.62−1.59 (m, 2H; CH_2) (Figure S2).

Synthesis of PEG-IO. PEG-IO was synthesized as described previously.[71] Briefly, BTTAA (2.4 mg in 120 μL of H_2O) and sodium ascorbate (NaAsc, 2 mg in 100 μL of H_2O) were added to a $CuSO_4$ solution (100 mM, 60 μL). Alkyne-imidazolium-oxime (22 mg) and NH_2-PEG_6-N_3 (20 mg in 300 μL DMF) were added to the solution. The reaction mixture was incubated at room temperature for 1 h. The product was purified by precipitation in ether/acetone = 10/1 four times and dried by a vacuum. Dark oil, 75% yield. ^{1}H NMR (400 MHz, MeOD-d4) δ 8.60 (s, 1H; CH), 7.94 (s, 1H, Ar H), 7.92 (s, 1H, Ar H), 7.81 (d, J = 3, 1H, Ar H), 7.49 (d, J = 3, 2H, Ar H), 7.33 (d, J = 6, 2H, Ar H), 5.59 (s, 2H; CH_2), 4.45 (t, J = 3, 2H; CH_2), 4.35 (t, J = 3, 2H; CH_2), 3.78 (s, 2H; CH_2), 3.50−3.44 (m, 24H; 12CH_2), 2.62 (d, J = 3, 2H, CH_2), 1.81−1.79 (m, 2H; CH_2), 1.59 (d, J = 3, 2H, CH_2) (Figure S2). PEG-IO was used as a standard for the calculation of oxime to BChE ratios of BChE-polymer-oxime conjugates.

Synthesis of Alkyne-Pyridinium-Oxime. Isonicotinaldehyde (50 mmol), hydroxylamine hydrochloride (55 mmol), and K_2CO_3 (7.6 g, 55 mmol) were mixed in 250 mL of MeOH at room temperature overnight. After the solvent was removed using a rotary evaporator, the residue was diluted with water (250 mL) and extracted with ethyl acetate (5 × 150 mL). The combined extract was washed with brine (2 × 150 mL) and dried over $MySO_4$. The solvent was removed using a rotary evaporator, and the product isonicotinaldehyde oxime was obtained in 84% yield.

Isonicotinaldehyde oxime (10 mmol) and 1,4-diiodobutane (30 mmol) were dissolved in 50 mL of ACN and stirred at room temperature for 5 days. The resulting precipitate was collected by filtration and then concentrated and added to 50 mL of ethyl acetate. We next collected and combined the precipitate and purified it using silica gel (EA/MeOH/HCOOH = 4/1/0.25) to generate the product 4-((hydroxyimino)methyl)-1-(4-iodobutyl)pyridin-1-ium iodide in 77% yield.

4-((Hydroxyimino)methyl)-1-(4-iodobutyl)pyridin-1-ium iodide (0.5 mmol) was dissolved in 5 mL of ACN and 400 μL of DMSO. *N*,*N*-Dimethylprop-2-yn-1-amine (1 mmol) was added to the ACN/DMSO solution and stirred at room temperature for 2 days. The solvent was removed by rotary evaporation. The product alkyne-pyridinium-oxime was purified by precipitation in ethyl acetate/acetone (2/1) three times and dried by vacuum. Yellow powder, 65% yield. ^{1}H NMR (400 MHz, MeOD-d4) δ 8.82 (d, J = 6, 2H, Ar H), 8.35 (s, 1H, Ar H), 8.19 (d, J = 6, 2H, Ar H), 4.68−4.63 (m, 2H; CH_2), 4.23 (d, J = 3, 2H, CH_2), 3.49−3.46 (m, 2H; CH_2), 3.23 (t, J = 3, 1H; CH), 3.15 (s, 6H; 2CH_3), 2.18−2.07 (m, 2H; CH_2), 1.91−1.87 (m, 2H; CH_2) (Figure S3).

Synthesis of PEG-PO. PEG-PO was synthesized as described previously.[71] Briefly, BTTAA (13 mg in 300 μL of H_2O) and sodium ascorbate (NaAsc, 20 mg in 200 μL of H_2O) were added to a $CuSO_4$ solution (100 mM, 300 μL). Alkyne-pyridinium-oxime (52 mg) and NH_2-PEG_3-N_3 (55 mg in 600 μL DMF) were then added to the solution, and the reaction mixture was incubated at room temperature overnight. The product was purified by precipitation in ether/acetone = 10/1 four times and dried by a vacuum. Dark oil, 53% yield. ^{1}H NMR (400 MHz, MeOD-d4) δ 8.82 (s, 1H; Ar H), 8.80 (s, 1H; Ar H), 8.34 (d, J = 3, 2H, Ar H), 8.17 (d, J = 6, 2H, Ar H), 4.69−4.62 (m, 6H; 3CH_2), 3.95 (t, J = 3, 2H, CH_2), 3.70 (t, J = 3, 2H, CH_2), 3.65−3.59 (m, 8H; 4CH_2), 3.35−3.32 (m, 2H; CH_2), 3.16 (t, J = 3, 2H, CH_2), 3.04 (s, 6H; 2CH_3), 2.08−2.03 (m, 2H; CH_2), 2.01−1.95 (m, 2H; CH_2) (Figure S3). PEG-PO was used as a standard for the calculation of oxime to BChE ratios of BChE-polymer-oxime conjugates.

Synthesis of BChE-Polymer-Oxime Conjugates. The BChE-PDMAA-N_3 conjugate was synthesized as described previously.[71] Alkyne-imidazolium-oxime (IO) or alkyne-pyridinium-oxime (PO) was attached to the side chains of BChE-PDMAA-N_3 conjugate by "click" chemistry.[74] NaAsc (10 mM × 35 μL), $CuSO_4$ (10 mM × 17.6 μL), and BTTAA (10 mM × 35 μL) in distilled water were added into a BChE-PDMAA-N_3 (27 μM BChE, 650 μL) solution. Alkyne-imidazolium-oxime or alkyne-pyridinium-oxime (50 mM) in distilled water was added in different oxime to BChE ratios (40-, 80-, or 160-fold). The reaction mixture was incubated at room temperature for 3 h. The BChE-PDMAA-OX conjugates were purified by ultrafiltration (50 kDa cutoff membrane) four times. The number of oximes per BChE monomer of the conjugates was determined by BCA assay and UV absorbance at 280 nm (Figure S1). BChE-PDMAA-OX conjugates were characterized by GPC and SDS-PAGE analysis.

Synthesis of PDMAA-IO and PDMAA-PO. To synthesize the azide containing copolymer, PDMAA-N_3, DMAA (1.20 mmol), MA-PEG_6-N_3 (60 μmol), and ATRP initiator (1 μmol) were mixed in 2 mL of PB buffer (50 mM, pH 7.4), sealed, and bubbled with argon for 30 min at room temperature. Deoxygenated Me_6TREN (8 μmol), $CuBr_2$ (3 μmol), and NaAsc (4 μmol) in distilled water (1 mL) were added to the initiator−monomer solution, sealed, and stirred for 2 h at room temperature. The copolymer PDMAA-N_3 was purified by dialysis (8 kDa cutoff membrane) in distilled water and lyophilization. The molecular weight (M_n) and dispersity ($Đ$) of PDMAA-N_3 were 64.4 kDa and 1.87, respectively (Figures S4 and S5). GPC calibration was based on poly(ethylene glycol) standards.

Alkyne-imidazolium-oxime or alkyne-pyridinium-oxime was attached to the side chains of PDMAA-N_3 conjugate by "click" chemistry to prepare PDMAA-IO or PDMAA-PO.[74] NaAsc (10 mM × 80 μL), $CuSO_4$ (10 mM × 40 μL), and BTTAA (10 mM × 80 μL) in distilled water were added into a PDMAA-N_3 (14 mg in 650 μL of H_2O) solution. Alkyne-imidazolium-oxime or alkyne-pyridinium-oxime (2 mg in 80 μL DMSO) was added and incubated at room temperature overnight. PDMAA-IO or PDMAA-PO was purified by ultrafiltration (30 kDa cutoff membrane) four times.

The oxime content of PDMAA-IO and PDMAA-PO, determined from the UV−vis spectra, was 12.5 and 4.5 wt %, respectively (Figures S1 and S4).

Activity Assay of BChE and BChE-PDMAA-OX Conjugates. BTC was used as a substrate to determine the activity of BChE and BChE-PDMAA-OX conjugates at room temperature. One milliliter of BTC (1 mM) and DTNB (Ellman assay reagent, 0.1 mM) in PB buffer (50 mM, pH 7.4) was added to a 1.5 mL cuvette. Native BChE or BChE-PDMAA-OX conjugate (20 nM protein, 100 μL) was then added to the cuvette.[75] The activity of BChE or BChE-PDMAA-OX conjugates was evaluated by monitoring BTC hydrolysis, resulting in an increase in absorbance at 412 nm from TNB (extinction coefficient of 14 000 M^{-1} cm^{-1}), using a Lambda 2 PerkinElmer UV−vis spectrophotometer.

Inhibition Assay of BChE and BChE-Polymer-Oxime Conjugates. BChE or BChE-PDMAA-OX conjugate (20 or 10 nM) was incubated with a 5-fold stoichiometric excess of EMP-MeCyC or CMP-MeCyC at room temperature. An aliquot was diluted 10 or 20 times in PB buffer (50 mM, pH 7.4) at specified time intervals. After addition of BTC (1 mM) and DTNB (0.1 mM), we measured the enzymatic activity of each group. The uninhibited BChE or BChE-PDMAA-OX conjugate was treated as 100% activity at the time zero. Activity evaluation was performed in PB buffer (50 mM, pH 7.4) by the Ellman assay using a Lambda 2 PerkinElmer UV−vis spectrophotometer.[75]

Flu-OPNAs Degradation Assay. A mixture of BChE, BChE-PDMAA-IO_{172} conjugate (or BChE-PDMAA-PO_{216} conjugate), and PDMAA-IO (or PDMAA-PO) at various ratios (protein 50 nM; Oxime/BChE = 43 or 54) was incubated with a 5-fold excess of EMP-MeCyC (or CMP-MeCyC) in PB buffer at pH 7.4. The total volume of the mixture was 100 μL. The fluorescence intensity (ex 400 nm; em 446 nm) was measured using a Bio-Tek Synergy H1 plate reader at specified time intervals.

Reactivation Assay of BChE and BChE-PDMAA-OX Conjugates. A reactivation assay was carried out with BChE or BChE-PDMAA-OX conjugates (1 μM) in 1 mg/mL bovine serum albumin (BSA)

https://dx.doi.org/10.1021/acs.biomac.0c00959
Biomacromolecules 2020, 21, 3867−3877

Table 1. Characterization of BChE-PDMAA-OX Conjugates

	Conjugate M_w [kDa]	Copolymer (3-Column GPC) M_w [kDa]	Copolymer (3-Column GPC) $Đ$ [M_w/M_n]	Oximes/BChE tetramer	Structure of IO/PO
BChE-PDMAA-IO:					
BChE-PDMAA-IO_{28}	2,636	88.3	1.7	28	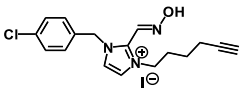
BChE-PDMAA-IO_{84}	2,660	89.2	1.7	84	
BChE-PDMAA-IO_{172}	2,700	90.7	1.7	172	IO
BChE-PDMAA-PO:					
BChE-PDMAA-PO_{44}	2,648	88.7	1.7	44	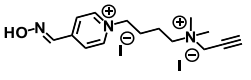
BChE-PDMAA-PO_{104}	2,676	89.9	1.7	104	
BChE-PDMAA-PO_{216}	2,736	92.1	1.7	216	PO

solution in PB buffer (50 mM, pH 6.0) that we mixed with a 10-fold molar excess of EMP-MeCyC or CMP-MeCyC in PB buffer (50 mM, pH 6.0) for 10 min. The completely inactive BChE or conjugates were transferred into an ultrafiltration tube (50 kDa cutoff membrane) to remove the excess of EMP-MeCyC or CMP-MeCyC (10 000*g* for 5 min, 3 times), then diluted 50-fold in PB buffer (50 mM, pH 8.0) at room temperature. At specified time intervals, the activities of BChE or conjugates were measured by Ellman assay using BTC (1 mM) and DTNB (0.1 mM). The activity of uninhibited BChE or conjugates was used to determine the 100% activity.

Inactivation and Reactivation Recycle of BChE-PDMAA-OX Conjugates. BChE-PDMAA-IO conjugates (1 μM) in 1 mg/mL bovine serum albumin (BSA) in PB buffer (50 mM, pH 6.0) solution was mixed with a 10-fold molar excess of EMP-MeCyC in PB buffer (50 mM, pH 6.0) for 10 min. The completely inactive conjugates were purified by ultrafiltration tube (50 kDa cutoff membrane, 10 000*g* for 5 min, 3 times), then diluted 50-fold in PB buffer (50 mM, pH 8.0) and incubated at room temperature for 200 min. The conjugates were buffer-exchanged with PB buffer (50 mM, pH 6.0) and concentrated to 1 μM, then mixed with a 10-fold molar excess of EMP-MeCyC in PB buffer (50 mM, pH 6.0) and incubated at room temperature for 10 min. The completely inactive conjugates were purified by ultrafiltration tube (50 kDa cutoff membrane, 10 000*g* for 5 min, 3 times), then diluted 50-fold in PB buffer (50 mM, pH 8.0) and incubated at room temperature for 200 min. The inactivation and reactivation cycle were repeated three times. At specified time intervals, the conjugate activity was measured by the Ellman assay using BTC (1 mM) and DTNB (0.1 mM) as substrates. The activity of uninhibited or activity recovered conjugates at pH 8.0 after 200 min was used to determine the 100% activity value.

Tertiary Structure-Based Prediction of NHS-ATRP Initiator Modification. The tertiary structure of BChE was downloaded from the Protein Data Bank (PDB code: 6I2T). In order of influence on initiator-amino group specificity, the following properties for each lysine residue and N-termini were determined: exposed surface area (ESA), steric hindrance, pK_a, secondary structure, local charge, and H-bonding (Table S1).[76]

RESULTS AND DISCUSSION

Synthesis and Characterization of BChE-Polymer-Oxime Conjugates. To synthesize BChE-polymer-oxime conjugates, an *N*-hydroxysuccinimide (NHS) ester modified ATRP initiator (NHS-Br) was reacted with accessible amine groups on the surface of BChE, generating the macroinitiator BChE-Br. On average, 6.5 initiators were attached to each BChE monomer.[71] To pinpoint where these modification sites were located, we employed a tertiary structure-based predictive model that we had previously developed to identify highly reactive amine groups on the surface BChE.[76] This approach enabled us to isolate the N-termini and a small group of lysine residues (K9, K60, K105, K190, and K558) as the likely sites of reaction with the ATRP initiators (Table 1). Azide-containing copolymers were grown from BChE-Br at fast-modified lysine residues and the N-termini by *in situ* ATRP with a neutral monomer, *N*,*N*-dimethylacrylamide (DMAA), in the presence of an azido monomer (MA-PEG_6-N_3) to generate BChE-PDMAA-N_3 conjugates, as described previously.[71] Copper catalyzed azide−alkyne cycloaddition "click" chemistry was then used to couple an alkyne-imidazolium-oxime or an alkyne-pyridinium-oxime to the azido-containing copolymers of BChE-PDMAA-N_3 conjugates (Figure 1). Stoichiometric alkyne-imidazolium-oxime (IO) or alkyne-pyridinium-oxime (PO) excesses of 40-fold, 80-fold, or 160-fold were used to modify BChE-PDMAA-N_3 in the preparation of BChE-PDMAA-OX conjugates (BChE-PDMAA-IO and BChE-PDMAA-PO). The BChE-PDMAA-OX conjugates were purified by ultrafiltration (50 kDa cutoff membrane), and the oxime to BChE ratios were determined using the bicinchoninic acid (BCA) assay and absorbance at 280 nm (Figure S1). The number of imidazolium-oximes per BChE tetramer was 28, 84, and 172 for BChE-PDMAA-IO conjugates (we refer to these conjugates as BChE-PDMAA-IO_{28}, BChE-PDMAA-IO_{84}, and BChE-PDMAA-IO_{172}, respectively). The number of pyridi-

https://dx.doi.org/10.1021/acs.biomac.0c00959
Biomacromolecules 2020, 21, 3867−3877

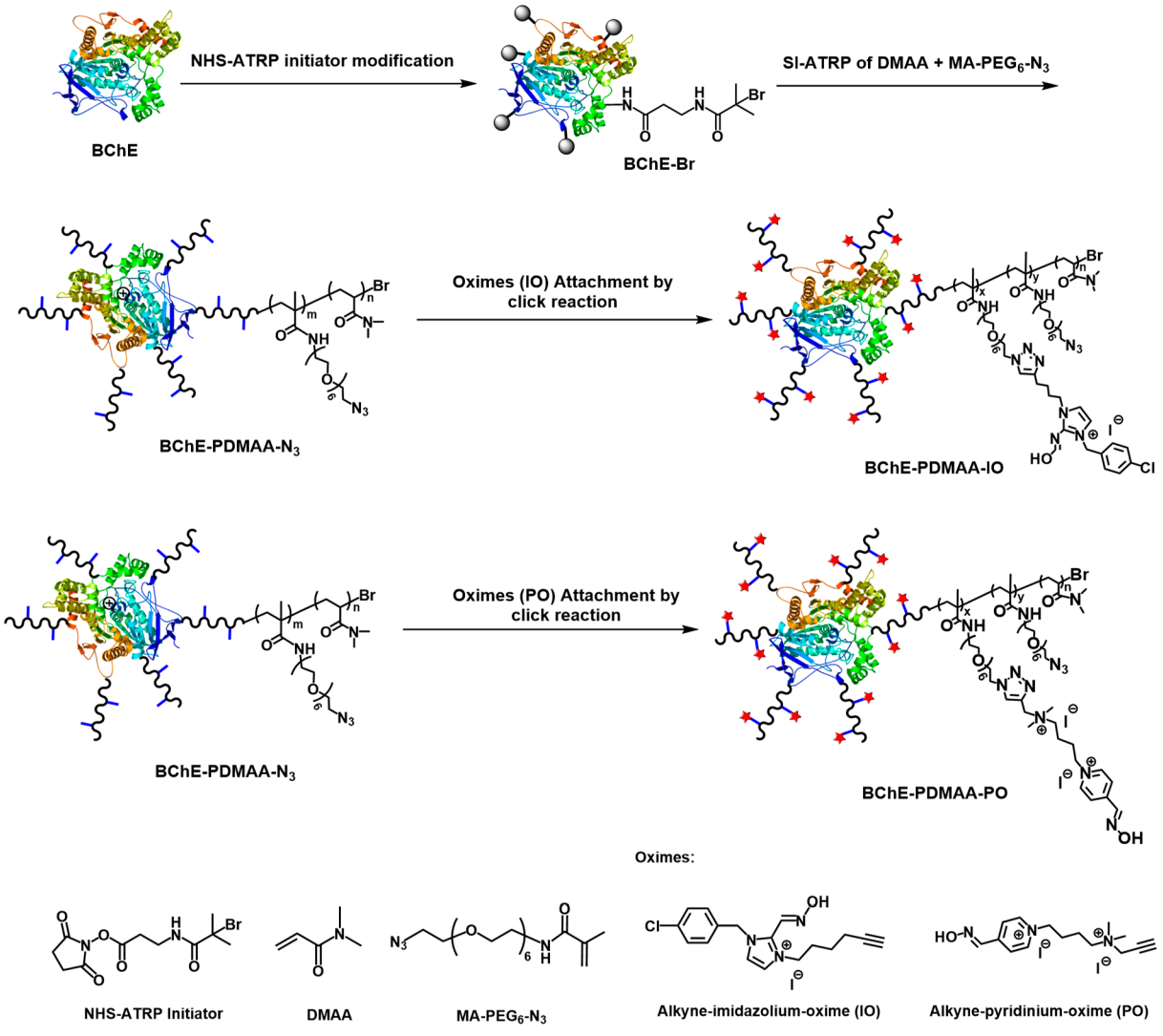

Figure 1. Synthesis of butyrylcholinesterase-polymer-oxime conjugates using atom-transfer radical polymerization (ATRP) and "click" chemistry. Additional acronyms: *N*-hydroxysuccinimide (NHS), *N*,*N*-dimethylacrylamide (DMAA), *N*-(20-azido-3,6,9,12,15,18-hexaoxaicosyl)-methacrylamide (MA-PEG$_6$-N$_3$), butyrylcholinesterase (BChE).

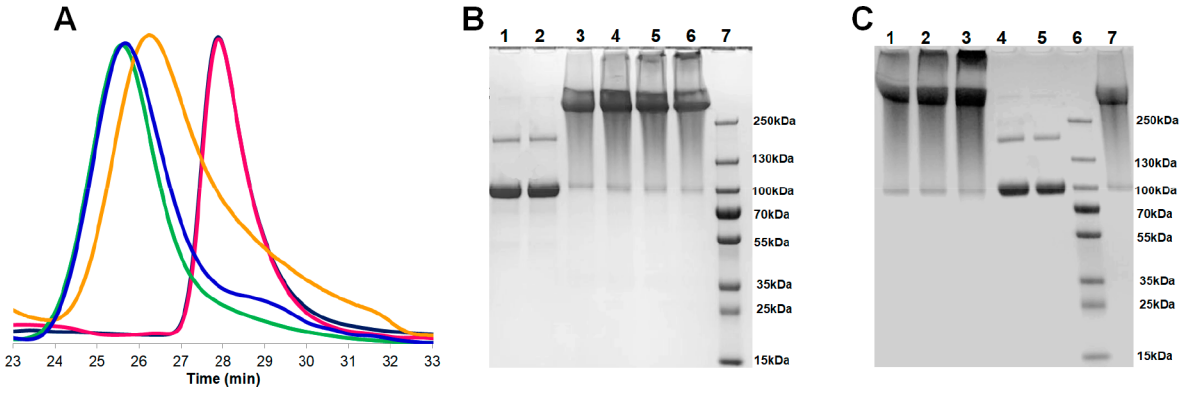

Figure 2. Characterization of BChE, BChE-Br, BChE-PDMAA-N$_3$, and BChE-PDMAA-OX conjugates. (A) GPC analysis of BChE (black curve), BChE-Br (red curve), BChE-PDMAA-N$_3$ (green curve), BChE-PDMAA-IO$_{84}$ (yellow curve), and BChE-PDMAA-PO$_{104}$ (blue curve) conjugates. (B) SDS-PAGE analysis of BChE, BChE-Br, BChE-PDMAA-N$_3$, and BChE-PDMAA-IO conjugates. Lane 1: BChE; Lane 2: BChE-Br; Lane 3: BChE-PDMAA-N$_3$; Lane 4: BChE-PDMAA-IO$_{28}$; Lane 5: BChE-PDMAA-IO$_{84}$; Lane 6: BChE-PDMAA-IO$_{172}$; Lane 7: Marker. (C) SDS-PAGE analysis of BChE, BChE-Br, BChE-PDMAA-N$_3$, and BChE-PDMAA-PO conjugates. Lane 1: BChE-PDMAA-PO$_{44}$; Lane 2: BChE-PDMAA-PO$_{104}$; Lane 3: BChE-PDMAA-PO$_{216}$; Lane 4: BChE-Br; Lane 5: BChE; Lane 6: Marker; Lane 7: BChE-PDMAA-N$_3$.

https://dx.doi.org/10.1021/acs.biomac.0c00959
Biomacromolecules 2020, 21, 3867−3877

nium-oximes per BChE tetramer was 44, 104, and 216 for BChE-PDMAA-PO conjugates BChE-PDMAA-PO_{44}, BChE-PDMAA-PO_{104}, and BChE-PDMAA-PO_{216}, respectively. The molecular weights and purities of the BChE-PDMAA-OX conjugates were compared by gel permeation chromatography (GPC) and sodium dodecyl sulfate polyacrylamide gel electrophoresis (SDS-PAGE) analysis (Table 1, Figure 2). It is important to note that there are no GPC standards for these kinds of protein−polymer conjugates, so we must be cautious when interpreting observed conjugate molecular weights. That said, GPC can be useful when interpreting the differences in apparent molecular weight between various conjugates.

We next investigated whether the BChE-PDMAA-OX conjugates retained bioactivity. Using *S*-butyrylthiocholine iodide (BTC) as a substrate (10 μM, pH 8.0), we compared conjugate activity to that of native BChE. For BChE-PDMAA-IO_{28}, BChE-PDMAA-IO_{84}, and BChE-PDMAA-IO_{172}, activity was inversely proportional to oxime content (76, 67, and 54%, respectively). The BChE-PDMAA-PO conjugates also exhibited reduced activity but with a less pronounced inverse dependence on oxime content (63, 48, and 48% for BChE-PDMAA-PO_{44}, BChE-PDMAA-PO_{104}, and BChE-PDMAA-PO_{216}, respectively) (Figure 3). Previous work lead us to

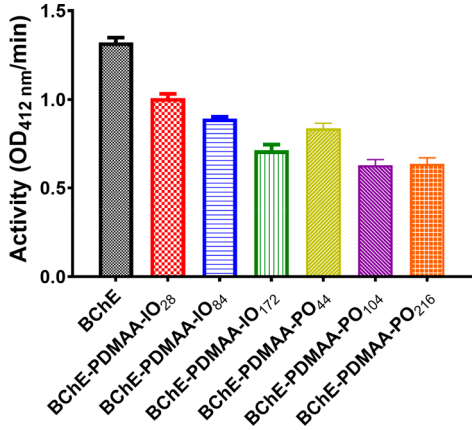

Figure 3. Enzymatic activity of BChE, BChE-PDMAA-IO, and BChE-PDMAA-PO conjugates at a single concentration of BTC in PB (50 mM) buffer at pH 8.0. Results are presented as mean values ± standard deviation (n = 3).

hypothesize that the activity loss of BChE-PDMAA-OX conjugates resulted from a combination of polymer attachment and reversible direct oxime inhibition of the enzyme.[23,71] In addition, Cu^{2+} and Cu-ligand complexes can inhibit cholinesterase activity.[77,78] Although previous reports on ChE reversible inhibition by copper ions are a concern, the extensive washing of the click reaction products eliminated copper-mediated inhibition. The alkyne-imidazolium-oxime had a BChE IC_{50} of approximately 1 μM (Figure S6) and the alkyne-pyridinium-oxime BChE IC_{50} was >50 μM (Figure S7). The BChE-PDMAA-OX conjugates reported herein were the highest activity BChE-polymer-oxime conjugates that we have studied to date. We recently determined the Michaelis−Menten kinetics for the BChE, BChE-Br, and BChE-PDMAA-N_3 starting materials.[71]

Because only negatively charged oximates can reactivate BChE active sites, it was important to determine the pK_a values for the monomeric alkyne-imidazolium-oxime and alkyne-pyridinium-oxime.[79] We used a spectroscopic assay and thereby surmised that the oximes groups on BChE-PDMAA-IO and BChE-PDMAA-PO had pK_a values of 8.35 and 8.38, respectively (Figure S8). Thus, at pH 6.0, the conjugates would be in their fully protonated oxime form and therefore would be unable to undergo either inter- or intramolecular reactivation. Therefore, to minimize any reactivation, we inhibited the BChE-polymer-oxime conjugates by fluorogenic OPNA (Flu-OPNA) analogues at pH 6.0 (vide infra).

Oxime Containing Copolymers Protect BChE against OPs. Two racemic Flu-OPNAs analogues, which were designed to be analogues of VX or cyclosarin after reaction with BChE, were used to inhibit BChE-polymer-oxime conjugates. The Flu-OPNAs contained either an ethyl (E) or cyclohexyl (C) O-alkyl attached to a methyl-phosphoryl (MP) moiety. The fluorescent moiety, 3-cyano-4-methyl-7-hydroxy coumarin (MeCyC-OH), was released upon reaction between the BChE active site serine and Flu-OPNAs (EMP-MeCyC or CMP-MeCyC) resulting in a significant and measurable increase in fluorescence intensity.[72] BChE-PDMAA-OX conjugates (10 or 20 nM) were exposed to a 5-fold stoichiometric excess of Flu-OPNAs in sodium phosphate buffer (pH 7.4, 50 mM), and the activity loss was measured over time by removing aliquots and performing an activity assay as described above. Following the addition of Flu-OPNAs, native BChE lost all activity within 10 min (Figure S9A). After exposure to EMP-MeCyC, BChE-PDMAA-IO_{28}, BChE-PDMAA-IO_{84}, and BChE-PDMAA-IO_{172} retained 7, 10, and 15% activity, respectively (Figure S9A). The BChE-PDMAA-PO_{44}, BChE-PDMAA-PO_{104}, and BChE-PDMAA-PO_{216} conjugates retained 27, 28, and 35% activity, respectively (Figure S9B). Thus, all the BChE-PDMAA-OX conjugates were all moderately resistant to inactivation by EMP-MeCyC with the degree of protection being proportional to oxime content and related to oxime structure. Imidazolium-oxime containing copolymers also protected BChE against CMP-MeCyC (Figure S10A), though the highest oxime content BChE-PDMAA-PO did not resist inactivation by EMP-MeCyC (Figure S10B). The BChE-PDMAA-OX conjugates were all inactivated eventually by a large excess of paraoxon (POX) (Figure S11).

To elucidate whether the protection of oxime containing BChE-PDMAA-OX conjugates against Flu-OPNAs was consistent with intramolecular and/or intermolecular interactions, inhibition was monitored in mixtures of native BChE, BChE-PDMAA-OX conjugates, and oxime containing copolymers (PDMAA-IO and PDMAA-PO) using the release of fluorescence (the leaving group is MeCyC-OH) upon covalent coupling of Flu-OPNAs to the enzyme (Figure 4). The total oxime content was kept constant at 172 and 216 equiv for BChE-PDMAA-IO and BChE-PDMAA-PO, respectively, delivering the oxime by polymer only or enzyme-linked oxime. The presence of free PDMAA-IO enhanced EMP-MeCyC hydrolysis. BChE-PDMAA-IO_{172} with no free PDMAA-IO had the lowest fluorescence intensity increase. The degree of fluorescence intensity increased steadily as the fraction of free PDMAA-IO increased over 20 min (Figure 4A). These data, when combined with control experiments, showed that free PDMAA-IO could protect BChE against EMP-MeCyC, thereby indicating that intermolecular protection accounted for the majority of the observed protection. A similar phenomenon was observed in the fluorescence monitoring assay of CMP-MeCyC mixed with BChE, PDMAA-PO, and BChE-PDMAA-PO_{216} (Figure 4B). CMP-

https://dx.doi.org/10.1021/acs.biomac.0c00959
Biomacromolecules 2020, 21, 3867−3877

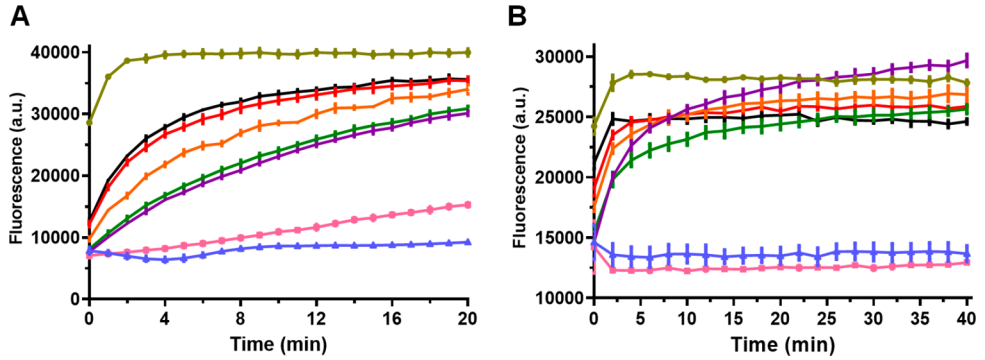

Figure 4. Time-course of Flu-OPNA (250 nM) degradation by mixtures of BChE, polymer-oxime, and BChE-PDMAA-OX conjugates in PB buffer at pH 7.4. (A) Fluorescence intensity of EMP-MeCyC mixed with BChE, PDMAA-IO, and BChE-PDMAA-IO_{172} (imidazolium-oxime/BChE tetramer = 172). (B) Fluorescence intensity of CMP-MeCyC mixed with BChE, PDMAA-PO, and BChE-PDMAA-PO_{216} (pyridinium-oxime/BChE tetramer = 216). Black curve: 100% BChE; red curve: 80% BChE + 20% BChE-PDMAA-IO_{172} (or BChE-PDMAA-PO_{216}); orange curve: 50% BChE + 50% BChE-PDMAA-IO_{172} (or BChE-PDMAA-PO_{216}); green curve: 20% BChE + 80% BChE-PDMAA-IO_{172} (or BChE-PDMAA-PO_{216}); purple curve: 100% BChE-PDMAA-IO_{172} (or BChE-PDMAA-PO_{216}); yellow curve: only BChE; pink curve: only PDMAA-IO; blue curve: PB buffer. Results are presented as mean values ± standard deviation (n = 3).

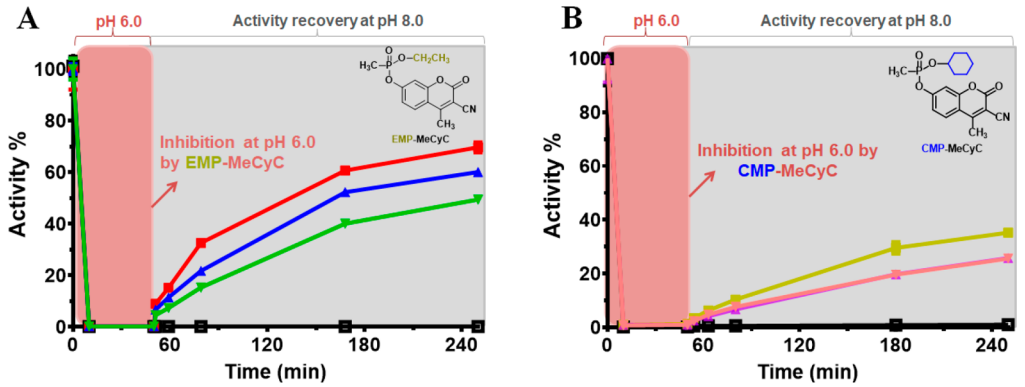

Figure 5. Reactivation assay of BChE-PDMAA-IO conjugates inhibited by EMP-MeCyC (A) and BChE-PDMAA-PO conjugates inhibited by CMP-MeCyC (B). BChE-PDMAA-IO, BChE-PDMAA-PO, or free BChE (1 μM) were inhibited by 10-fold excess of Flu-OPNAs in PB buffer at pH 6.0 for 10 min. The excess Flu-OPNAs were removed and then diluted 50-fold in PB buffer at pH 8.0. Black curve: BChE; green curve: BChE-PDMAA-IO_{28}; blue curve: BChE-PDMAA-IO_{84}; red curve: BChE-PDMAA-IO_{172}; pink curve: BChE-PDMAA-PO_{44}; purple curve: BChE-PDMAA-PO_{104}; yellow curve: BChE-PDMAA-PO_{216}. Results are presented as mean values ± standard deviation (n = 3).

MeCyC did not significantly hydrolyze in PB buffer at pH 7.4 at room temperature over 40 min. PDMAA-PO addition reduced the fluorescence intensity of MeCyC-OH (the leaving group), and the fluorescence intensity of CMP-MeCyC did not increase upon BChE addition indicating complete inactivation of the active site. Because we know that native BChE stoichiometrically reacts with OPNAs in a 1 to 1 ratio and the fluorescence intensity of CMP-MeCyC with BChE-PDMAA-PO was higher than that with BChE after 40 min, we deduced that one molecule of BChE-PDMAA-PO could scavenge approximately 1.4 molecules of CMP-MeCyC based on the difference of fluorescence intensity between 100% BChE group and 100% BChE-PDMAA-PO_{216} group.

To discover whether or not oxime side chains reacted directly with EMP-MeCyC and/or CMP-MeCyC, we monitored the fluorescence intensity of Flu-OPNAs after the addition of free imidazolium- or pyridinium-oximes. Alkyne-imidazolium-oxime addition enhanced the fluorescence of the MeCyC-OH moiety released from EMP-MeCyC and CMP-MeCyC (Figure S12). We observed a reduction in the fluorescence of EMP-MeCyC and CMP-MeCyC after the addition of alkyne-pyridinium-oxime (Figure S12B). EMP-MeCyC spontaneously hydrolyzed in PB buffer at pH 7.4 at room temperature (Figure S12A). The decreased inhibition rates of the conjugates by EMP-MeCyC and CMP-MeCyC could have been caused by a direct reaction between the imidazolium-oxime and Flu-OPNAs. We were able to rule out, however, that the protection by pyridinium-oxime containing copolymer on the surface of BChE-polymer-oxime conjugates was related to a direct reaction between pyridinium-oxime and CMP-MeCyC. The reversible inhibition of the BChE active site by pyridinium-oxime apparently masked the active site toward inhibition by CMP-MeCyC.

Reactivation of Flu-OPNA-Inhibited BChE-PDMAA-OX Conjugates. To determine whether free alkyne-imidazolium-oxime and alkyne-pyridinium-oxime were effective reactivators of BChE-EMP and BChE-CMP covalent complexes, Flu-OPNA-inhibited BChE was treated with a 25 000-fold stoichiometric excess of free oxime (0.5 mM) (Figure S13). More than 40% of EMP-MeCyC- and CMP-MeCyC-inhibited BChE activity was recovered after the addition of alkyne-pyridinium-oxime within 24 h (Figure S13). Addition of 2-PAM (0.5 mM), a positive control reagent, restored more than 65% activity over the same time period. There was no significant reactivation after the addition of the same amount of alkyne-imidazolium-oxime. Alkyne-imidazo-

https://dx.doi.org/10.1021/acs.biomac.0c00959
Biomacromolecules 2020, 21, 3867−3877

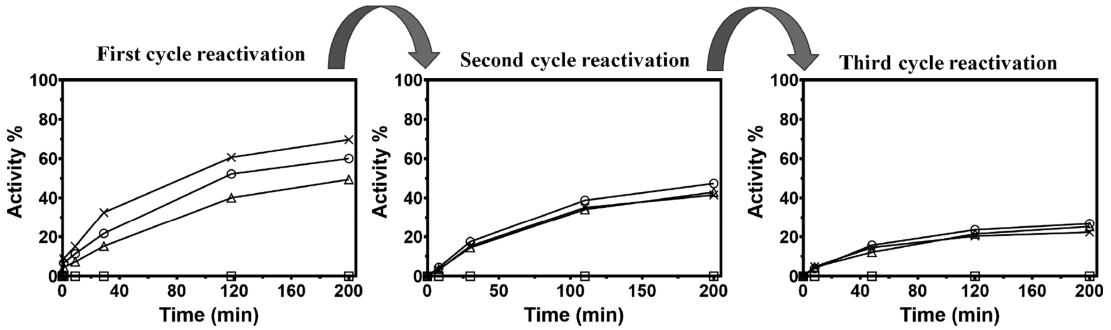

Figure 6. Inactivation and reactivation cycles of EMP-MeCyC-inhibited BChE-PDMAA-IO conjugates. ×: BChE-PDMAA-IO_{172}; ○: BChE-PDMAA-IO_{84}; △: BChE-PDMAA-IO_{28}; □: BChE. Results are presented as mean values ± standard deviation (n = 3).

lium-oxime had an IC_{50} of 1 μM (Figure S6). The active site of BChE, inhibited by Flu-OPNA, may be reactivated by the nucleophilic attack of alkyne-imidazolium-oxime but reversibly inhibited by excess oxime. To determine whether alkyne-imidazolium-oxime could restore the activity of Flu-OPNA-inhibited BChE, EMP-MeCyC-inhibited BChE was treated with different concentrations of alkyne-imidazolium-oxime. Lower concentrations of alkyne-imidazolium-oxime induced the reactivation of EMP-MeCyC inhibited BChE. More than 25% of enzyme activity was recovered 5 h after the addition of 2 μM alkyne-imidazolium-oxime, whereas a higher concentration of alkyne-imidazolium-oxime reactivated less than 25% of the activity due to reversible inhibition of BChE (Figure S14).

The degree to which the polymer-bound oxime could reactivate Flu-OPNA-inhibited BChE-PDMAA-OX conjugates was determined by first inhibiting the enzyme at low pH (6.0) and then tracking recovery of activity at high pH (8.0).[71] At pH 6.0, more than 2 units below the pK_a of alkyne-imidazolium-oxime and alkyne-pyridinium-oxime, we were able to inhibit the BChE active site of the BChE-PDMAA-OX conjugates without reactivation or interference by the polymer oxime side chains. BChE-PDMAA-OX conjugates and native BChE lost all activity after being mixed with a 10-fold molar excess of Flu-OPNAs at pH 6.0 within 10 min. The EMP-BChE-PDMAA-OX or CMP-BChE-PDMAA-OX conjugates were purified by removing excess Flu-OPNAs by ultrafiltration. Fluorescence intensity analysis showed that more than 99% of free Flu-OPNAs were removed after three cycles of ultrafiltration (Figure S15). The EMP-BChE-PDMAA-OX or CMP-BChE-PDMAA-OX conjugates were then diluted 50-fold in PB buffer at pH 8.0, and reactivation was measured using the Ellman assay with BTC as the substrate at pH 8.0 (Figure 5).

The degree of reactivation was determined relative to the respective initial activity of native BChE or a given BChE-PDMAA-OX conjugate in the assay. After complete inactivation by EMP-MeCyC, the combination of intra- and intermolecular reactivation was proportional to the oxime content of the polymer for the BChE-PDMAA-IO conjugates (Figure 5A). BChE-PDMAA-PO conjugates also recovered significant activity but with a less pronounced dependence on oxime content (Figure 5B). Prolonging the reactivation time to 24 h at pH 8.0, for the highest oxime content conjugates, resulted in dramatic levels of reactivation (84% for BChE-PDMAA-IO and 55% for BChE-PDMAA-PO) (Figure S16).

We next challenged the performance of imidazolium-oxime containing BChE-PDMAA-IO conjugates as catalytic bioscavengers against VX using the fluorogenic analogue EMP-MeCyC. The enzyme−polymer conjugates were inactivated with a 10-fold molar excess of EMP-MeCyC in PB buffer at pH 6.0; then, after ultrafiltration, we followed the reactivation at pH 8.0 for 200 min. At the end of the reactivation cycle, we readjusted the pH to 6.0 and again challenged the conjugates with another 10-fold molar excess of EMP-MeCyC. The entire process was repeated three times to determine whether the conjugates could self-reactivate after multiple challenges. In the second and third reactivation cycles, significant activity was recovered for all of the conjugates. We did observe a gradual decrease in the maximal reactivation levels at each consecutive cycle for BChE-PDMMA-IO_{172} conjugate, from 70% to 45% and 20% maximal activity recovery during the first, second, and third inhibition/reactivation cycles, respectively (Figure 6). This gradual decline in maximal reactivation level may stem from slow aging of inhibited conjugate active site. The distance of each oxime from the active site of the enzyme would likely influence the ability of a particular oxime to reactivate BChE. The decrease in maximal reactivation level in each inhibition-reactivation cycle could have been the result of a decrease in the concentration of active oximate ions that upon each reactivation reaction cycle would have been consumed and transformed into nitrile moieties (instead of the original aldoxime moieties).[80] Location-specific reactivation, and how it couples with cholinesterase aging, is beyond the scope of this manuscript but will be an important area for future study. The significant reactivation levels with inhibited conjugate after three inhibition/reactivation cycles were consistent, however, with catalytic reactivation of OPNA-inhibited BChE by matrix-conjugated oximes. In totality, these data demonstrated that covalent modification with imidazolium-oxime containing copolymers on the surface of BChE could catalytically decontaminate VX, even when the number of oximes per BChE tetramer molecule was as low as 28.

CONCLUSIONS

BChE-PDMAA-OX conjugates, synthesized by *in situ* ATRP and click chemistry with imidazolium-oxime and pyridinium-oxime side chains, were remarkable self-reactivators after repeated challenges with organophosphate inhibitors. The catalytic activity of these functional BChE-PDMAA-OX conjugates was dependent on the number of oximes per BChE molecule. The conjugates exhibited both inter- and intramolecular protection against fluorescent analogues of VX and cyclosarin, and functional enzyme activity in the presence of these OPs was prolonged by the conjugated polymer-oximes. After complete inactivation by EMP-MeCyC and

https://dx.doi.org/10.1021/acs.biomac.0c00959
Biomacromolecules 2020, 21, 3867−3877

CMP-MeCyC at a low pH (6.0), the conjugates recovered up to 84 and 55% activity respectively after self-reactivation pH (8.0) within 5−6 h. Imidazolium-oxime containing conjugates achieved three cycles of inhibition and autoreactivation, demonstrating high-performance decontamination bioscavenging.

■ ASSOCIATED CONTENT

Supporting Information

The Supporting Information is available free of charge at https://pubs.acs.org/doi/10.1021/acs.biomac.0c00959.

Complete data set, working curves, synthesis schemes, UV−vis absorbance spectrum, additional GPC data, fluorescence assay, activity assay, inhibition assay, and reactivation assay (PDF)

■ AUTHOR INFORMATION

Corresponding Author

Alan J. Russell − *Center for Polymer-Based Protein Engineering, Department of Chemical Engineering, and Department of Chemistry, Carnegie Mellon University, Pittsburgh, Pennsylvania 15213, United States;* orcid.org/0000-0001-5101-4371; Email: alanrussell@cmu.edu; Fax: 412-268-5229

Authors

Libin Zhang − *Center for Polymer-Based Protein Engineering, Carnegie Mellon University, Pittsburgh, Pennsylvania 15213, United States*

Hironobu Murata − *Center for Polymer-Based Protein Engineering, Carnegie Mellon University, Pittsburgh, Pennsylvania 15213, United States*

Gabriel Amitai − *Wohl Drug Discovery Institute, Nancy and Stephen Grand Israel National Center for Personalized Medicine (G-INCPM), Weizmann Institute of Science, Rehovot 760001, Israel*

Paige N. Smith − *Department of Biological Sciences, Carnegie Mellon University, Pittsburgh, Pennsylvania 15213, United States*

Krzysztof Matyjaszewski − *Center for Polymer-Based Protein Engineering, Department of Chemical Engineering, and Department of Chemistry, Carnegie Mellon University, Pittsburgh, Pennsylvania 15213, United States;* orcid.org/0000-0003-1960-3402

Complete contact information is available at: https://pubs.acs.org/10.1021/acs.biomac.0c00959

Author Contributions

L.Z.: conceptualization, methodology, software, writing the original draft, and data curation. H.M.: methodology. G.A.: conceptualization, review, and editing. P.N.S.: software and data curation. K.M.: supervision, review, and editing. A.J.R.: supervision, funding acquisition, review, and editing.

Funding

The authors acknowledge financial support provided by DTRA grant: HDTRA1-18-1-0028 Carnegie Mellon FRBAA14-BR-TA7-G19-2-0124.

Notes

The authors declare the following competing financial interest(s): A.R. and K.M. have founded a company that is commercializing protein-ATRP.

■ ACKNOWLEDGMENTS

The authors thank Dr. Roberto Gil and members of the NMR facility (Center for Molecular Analysis, Carnegie Mellon University) for their assistance with NMR spectroscopy, which was partially supported by the NSF (CHE-0130903, CHE-1039870, and CHE-1726525). We thank Dr. Oksana Lockridge (University of Nebraska, Medical Center) for kindly providing human BChE isolated from human plasma.

■ REFERENCES

(1) Gupta, R. C. *Handbook of Toxicology of Chemical Warfare Agents*, 3rd ed.; Academic Press-Elsevier: London, 2020.

(2) Balali-Mood, M.; Balali-Mood, K. Neurotoxic disorders of organophosphorus compounds and their managements. *Arch. Iran. Med.* **2008**, *11*, 65−89.

(3) Ohbu, S.; Yamashina, A.; Takasu, N.; Yamaguchi, T.; Murai, T.; Nakano, K.; Matsui, Y.; Mikami, R.; Sakurai, K.; Hinohara, S. Sarin poisoning on Tokyo subway. *South. Med. J.* **1997**, *90*, 587−600.

(4) Nagao, M.; Takatori, T.; Matsuda, Y.; Nakajima, M.; Iwase, H.; Iwadate, K. Definitive evidence for the acute sarin poisoning diagnosis in the Tokyo subway. *Toxicol. Appl. Pharmacol.* **1997**, *144*, 198−203.

(5) Yanagisawa, N.; Morita, H.; Nakajima, T. Sarin experiences in Japan: Acute toxicity and long-term effects. *J. Neurol. Sci.* **2006**, *249*, 76−85.

(6) Eddleston, M. Novel Clinical Toxicology and Pharmacology of Organophosphorus Insecticide Self-Poisoning. *Annu. Rev. Pharmacol. Toxicol.* **2019**, *59*, 341−360.

(7) Munro, N. Toxicity of the organophosphate chemical warfare agents GA, GB, and VX: implications for public protection. *Environ. Health Perspect.* **1994**, *102* (1), 18−38.

(8) Lotti, M. The Pathogenesis of Organophosphate Polyneuropathy. *Crit. Rev. Toxicol.* **1992**, *21* (6), 465−487.

(9) Voicu, V. A.; Thiermann, H.; Radulescu, F. S.; Mircioiu, C.; Miron, D. S. The Toxicokinetics and Toxicodynamics of Organophosphonates versus the Pharmacokinetics and Pharmacodynamics of Oxime Antidotes: Biological Consequences. *Basic Clin. Pharmacol. Toxicol.* **2010**, *106* (2), 73−85.

(10) Chambers, H. W. *Organophosphorus Compounds: An Overview, in Organophosphates: Chemistry, Fate, and Metabolism*; Chambers, J. E., Levi, P. E., Eds.; Academic Press: San Diego, CA, 1992, pp 3−17.

(11) Tochigi, M.; Umekage, T.; Otani, T.; Kato, T.; Iwanami, A.; Asukai, N.; Sasaki, T.; Kato, N. Serum cholesterol, uric acid and cholinesterase in victims of the Tokyo subway sarin poisoning: A relation with post-traumatic stress disorder. *Neurosci. Res.* **2002**, *44* (3), 267−272.

(12) Sit, R. K.; Radic, Z.; Gerardi, V.; Zhang, L.; Garcia, E.; Katalinic, M.; Amitai, G.; Kovarik, Z.; Fokin, V. V.; Sharpless, K. B.; Taylor, P. New Structural Scaffolds for Centrally Acting Oxime Reactivators of Phosphylated Cholinesterases. *J. Biol. Chem.* **2011**, *286* (22), 19422−19430.

(13) Milatovic, D.; Gupta, R. C.; Aschner, M. Anticholinesterase toxicity and oxidative stress. *Sci. World J.* **2006**, *6*, 295−310.

(14) Thiermann, H.; Worek, F.; Kehe, K. Limitations and challenges in treatment of acute chemical warfare agent poisoning. *Chem.-Biol. Interact.* **2013**, *206* (3), 435−443.

(15) Shih, T. M.; Guarisco, J. A.; Myers, T. M.; Kan, R. K.; McDonough, J. H. The oxime pro-2-PAM provides minimal protection against the CNS effects of the nerve agents sarin, cyclosarin, and VX in guinea pigs. *Toxicol. Mech. Methods* **2011**, *21* (1), 53−62.

(16) Wilson, I. B.; Ginsburg, S. A powerful reactivator of alkylphosphate-inhibited acetylcholinesterase. *Biochim. Biophys. Acta* **1955**, *18* (1), 168−170.

(17) Worek, F.; Thiermann, H. The value of novel oximes for treatment of poisoning by organophosphorus compounds. *Pharmacol. Ther.* **2013**, *139* (2), 249−259.

(18) Jokanovic, M.; Maksimovic, M.; Kilibarda, V.; Jovanovic, D.; Savic, D. Oxime-induced reactivation of acetylcholinesterase inhibited by phosphoramidates. *Toxicol. Lett.* **1996**, *85* (1), 35−39.
(19) Worek, F.; Kirchner, T.; Backer, M.; Szinicz, L. Reactivation by various oximes of human erythrocyte acetylcholinesterase inhibited by different organophosphorus compounds. *Arch. Toxicol.* **1996**, *70* (8), 497−503.
(20) Wong, L.; Radic, Z.; Bruggemann, R. J. M.; Hosea, N.; Berman, H. A.; Taylor, P. Mechanism of oxime reactivation of acetylcholinesterase analyzed by chirality and mutagenesis. *Biochemistry* **2000**, *39* (19), 5750−5757.
(21) Grifantini, M.; Stein, M. L.; Martelli, S. Structure-activity relationships in reactivators of organophosphorus-inhibited acetylcholinesterase. V. Quaternary salts of hydroxyiminomethylimidazoles. *J. Pharm. Sci.* **1972**, *61* (4), 631−633.
(22) Koolpe, G. A.; Lovejoy, S. M.; Goff, D. A.; Lin, K. Y.; Leung, D. S.; Bedford, C. D.; Musallam, H. A.; Koplovitz, I.; Harris, R. N. Quaternary salts of 2-[(hydroxyimino)methyl]imidazole. 5. Structure-activity relationships for side-chain nitro-, sulfone-, amino-, and aminosulfonyl-substituted analogues for therapy against anticholinesterase intoxication. *J. Med. Chem.* **1991**, *34* (4), 1368−1376.
(23) Katalinic, M.; Hrvat, N. M.; Baumann, K.; Pipercic, S. M.; Makaric, S.; Tomic, S.; Jovic, O.; Hrenar, T.; Milicevic, A.; Jelic, D.; Zunec, S.; Primozic, I.; Kovarik, Z. A comprehensive evaluation of novel oximes in creation of butyrylcholinesterase-based nerve agent bioscavengers. *Toxicol. Appl. Pharmacol.* **2016**, *310*, 195−204.
(24) Sit, R. K.; Fokin, V. V.; Amitai, G.; Sharpless, K. B.; Taylor, P.; Radic, Z. Imidazole Aldoximes Effective in Assisting Butyrylcholinesterase Catalysis of Organophosphate Detoxification. *J. Med. Chem.* **2014**, *57* (4), 1378−1389.
(25) Simeon-Rudolf, V.; Reiner, E.; Skrinjaric-Spoljar, M.; Radic, B.; Lucic, A.; Primozic, I.; Tomic, S. Quinuclidinium-imidazolium compounds: synthesis, mode of interaction with acetylcholinesterase and effect upon Soman intoxicated mice. *Arch. Toxicol.* **1998**, *72* (5), 289−295.
(26) Reiner, E.; Simeon-Rudolf, V. Pyridinium, imidazolium and quinuclidinium compounds: toxicity and antidotal effects against the nerve agents Tabun and Soman. *Arh. Hig. Rada toksikol.* **2006**, *57* (2), 171−179.
(27) Cochran, R.; Kalisiak, J.; Kucukkilinc, T.; Radic, Z.; Garcia, E.; Zhang, L. M.; Ho, K. Y.; Amitai, G.; Kovarik, Z.; Fokin, V. V.; Sharpless, K. B.; Taylor, P. Oxime-assisted Acetylcholinesterase Catalytic Scavengers of Organophosphates That Resist Aging. *J. Biol. Chem.* **2011**, *286* (34), 29718−29724.
(28) Voicu, V.; Radulescu, F. S.; Medvedovici, A. Relationships between the antidotal efficacy and structure, PK/PD parameters and bio-relevant molecular descriptors of AChE reactivating oximes: inclusion and integration to biopharmaceutical classification systems. *Expert Opin. Drug Metab. Toxicol.* **2015**, *11* (1), 95−109.
(29) Voicu, V. A.; Bajgar, J.; Medvedovici, A.; Radulescu, F. S.; Miron, D. S. Pharmacokinetics and pharmacodynamics of some oximes and associated therapeutic consequences: a critical review. *J. Appl. Toxicol.* **2010**, *30* (8), 719−729.
(30) Masson, P.; Nachon, F. Cholinesterase reactivators and bioscavengers for pre- and post-exposure treatments of organophosphorus poisoning. *J. Neurochem.* **2017**, *142*, 26−40.
(31) Raveh, L.; Grauer, E.; Grunwald, J.; Cohen, E.; Ashani, Y. The stoichiometry of protection against soman and VX toxicity in monkeys pretreated with human butyrylcholinesterase. *Toxicol. Appl. Pharmacol.* **1997**, *145* (1), 43−53.
(32) Wolfe, A. D.; Blick, D. W.; Murphy, M. R.; Miller, S. A.; Gentry, M. K.; Hartgraves, S. L.; Doctor, B. P. Use of cholinesterases as pretreatment drugs for the protection of rhesus monkeys against soman toxicity. *Toxicol. Appl. Pharmacol.* **1992**, *117* (2), 189−193.
(33) Ashani, Y.; Shapira, S.; Levy, D.; Wolfe, A. D.; Doctor, B. P.; Raveh, L. Butyrylcholinesterase and acetylcholinesterase prophylaxis against soman poisoning in mice. *Biochem. Pharmacol.* **1991**, *41* (1), 37−41.
(34) Doctor, B. P.; Raveh, L.; Wolfe, A. D.; Maxwell, D. M.; Ashani, Y. Enzymes as pretreatment drugs for organophosphate toxicity. *Neurosci. Biobehav. Rev.* **1991**, *15* (1), 123−128.
(35) Wolfe, A. D.; Rush, R. S.; Doctor, B. P.; Koplovitz, I.; Jones, D. Acetylcholinesterase prophylaxis against organophosphate toxicity. *Fundam. Appl. Toxicol.* **1987**, *9* (2), 266−270.
(36) Kovarik, Z.; Katalinic, M.; Sinko, G.; Binder, J.; Holas, O.; Jung, Y. S.; Musilova, L.; Jun, D.; Kuca, K. Pseudo-catalytic scavenging: Searching for a suitable reactivator of phosphorylated butyrylcholinesterase. *Chem.-Biol. Interact.* **2010**, *187* (1−3), 167−171.
(37) Guven, M.; Sungur, M.; Eser, B.; Sari, I.; Altuntas, F. The effects of fresh frozen plasma on cholinesterase levels and outcomes in patients with organophosphate poisoning. *J. Toxicol., Clin. Toxicol.* **2004**, *42* (5), 617−623.
(38) Mumford, H.; Price, M. E.; Lenz, D. E.; Cerasoli, D. M. Post-exposure therapy with human butyrylcholinesterase following percutaneous VX challenge in guinea pigs. *Clin. Toxicol.* **2011**, *49* (4), 287−297.
(39) Lockridge, O.; Schopfer, L. M.; Winger, G.; Woods, J. H. Large scale purification of butyrylcholinesterase from human plasma suitable for injection into monkeys; a potential new therapeutic for protection against cocaine and nerve agent toxicity. *J. Med. Chem. Biol. Radiol.* **2005**, *3*, nihms5095.
(40) Saxena, A.; Sun, W.; Luo, C. Y.; Doctor, B. P. Human serum butyrylcholinesterase: In vitro and in vivo stability, pharmacokinetics, and safety in mice. *Chem.-Biol. Interact.* **2005**, *157*, 199−203.
(41) Ostergaard, D.; Vibymogensen, J.; Hanel, H. K.; Skovgaard, L. T. Half-life of plasma cholinesterase. *Acta Anaesthesiol. Scand.* **1988**, *32*, 266−269.
(42) Grunwald, J.; Marcus, D.; Papier, Y.; Raveh, L.; Pittel, Z.; Ashani, Y. Large-scale purification and long-term stability of human butyrylcholinesterase: A potential bioscavenger drug. *J. Biochem. Biophys. Methods* **1997**, *34* (2), 123−135.
(43) Das, P. K.; Liddell, J. Purification and properties of human serum cholinesterase. *Biochem. J.* **1970**, *116* (5), 875−881.
(44) Ralston, J. S.; Main, A. R.; Kilpatrick, B. F.; Chasson, A. L. Use of procainamide gels in the purification of human and horse serum cholinesterases. *Biochem. J.* **1983**, *211* (1), 243−250.
(45) Muensch, H.; Goedde, H. W.; Yoshida, A. Human-serum cholinesterase subunits and number of active sites of the major componen. *Eur. J. Biochem.* **1976**, *70* (1), 217−223.
(46) Lockridge, O. Review of human butyrylcholinesterase structure, function, genetic variants, history of use in the clinic, and potential therapeutic uses. *Pharmacol. Ther.* **2015**, *148*, 34−46.
(47) Genovese, R. F.; Sun, W.; Johnson, C. C.; di Targiani, R. C.; Doctor, B. P.; Saxena, A. Safety of Administration of Human Butyrylcholinesterase and its Conjugates with Soman or VX in Rats. *Basic Clin. Pharmacol. Toxicol.* **2009**, *106* (5), 428−434.
(48) Ashani, Y.; Pistinner, S. Estimation of the upper limit of human butyrylcholinesterase dose required for protection against organophosphates toxicity: A mathematically based toxicokinetic model. *Toxicol. Sci.* **2004**, *77* (2), 358−367.
(49) Vanparijs, N.; Maji, S.; Louage, B.; Voorhaar, L.; Laplace, D.; Zhang, Q.; Shi, Y.; Hennink, W. E.; Hoogenboom, R.; De Geest, B. G. Polymer-protein conjugation via a 'grafting to' approach - a comparative study of the performance of protein-reactive RAFT chain transfer agents. *Polym. Chem.* **2015**, *6* (31), 5602−5614.
(50) Li, M.; De, P.; Gondi, S. R.; Sumerlin, B. S. Responsive polymer-protein bioconjugates prepared by RAFT polymerization and copper-catalyzed azide-alkyne click chemistry. *Macromol. Rapid Commun.* **2008**, *29* (12−13), 1172−1176.
(51) Grover, G. N.; Maynard, H. D. Protein-polymer conjugates: synthetic approaches by controlled radical polymerizations and interesting applications. *Curr. Opin. Chem. Biol.* **2010**, *14* (6), 818−827.
(52) Li, M.; De, P.; Li, H. M.; Sumerlin, B. S. Conjugation of RAFT-generated polymers to proteins by two consecutive thiol-ene reactions. *Polym. Chem.* **2010**, *1* (6), 854−859.

https://dx.doi.org/10.1021/acs.biomac.0c00959
Biomacromolecules 2020, 21, 3867−3877

(53) Ilyushin, D. G.; Smirnov, I. V.; Belogurov, A. A.; Dyachenko, I. A.; Zharmukhamedova, T. I.; Novozhilova, T. I.; Bychikhin, E. A.; Serebryakova, M. V.; Kharybin, O. N.; Murashev, A. N.; Anikienko, K. A.; Nikolaev, E. N.; Ponomarenko, N. A.; Genkin, D. D.; Blackburn, G. M.; Masson, P.; Gabibov, A. G. Chemical polysialylation of human recombinant butyrylcholinesterase delivers a long-acting bioscavenger for nerve agents in vivo. *Proc. Natl. Acad. Sci. U. S. A.* **2013**, *110* (4), 1243−1248.
(54) Terekhov, S.; Smirnov, I.; Bobik, T.; Shamborant, O.; Zenkova, M.; Chernolovskaya, E.; Gladkikh, D.; Murashev, A.; Dyachenko, I.; Palikov, V.; Palikova, Y.; Knorre, V.; Belogurov, A.; Ponomarenko, N.; Blackburn, G. M.; Masson, P.; Gabibov, A. A novel expression cassette delivers efficient production of exclusively tetrameric human butyrylcholinesterase with improved pharmacokinetics for protection against organophosphate poisoning. *Biochimie* **2015**, *118*, 51−59.
(55) Terekhov, S. S.; Smirnov, I. V.; Shamborant, O. G.; Bobik, T. V.; Ilyushin, D. G.; Murashev, A. N.; Dyachenko, I. A.; Palikov, V. A.; Knorre, V. D.; Belogurov, A. A.; Ponomarenko, N. A.; Kuzina, E. S.; Genkin, D. D.; Masson, P.; Gabibov, A. G. Chemical Polysialylation and In Vivo Tetramerization Improve Pharmacokinetic Characteristics of Recombinant Human Butyrylcholinesterase-Based Bioscavengers. *Acta Naturae* **2015**, *7* (4), 136−141.
(56) Rosenberg, Y. J.; Saxena, A.; Sun, W.; Jiang, X. M.; Chilukuri, N.; Luo, C. J.; Doctor, B. P.; Lee, K. D. Demonstration of in vivo stability and lack of immunogenicity of a polyethyleneglycol-conjugated recombinant CHO-derived butyrylcholinesterase bioscavenger using a homologous macaque model. *Chem.-Biol. Interact.* **2010**, *187* (1−3), 279−286.
(57) Lele, B. S.; Murata, H.; Matyjaszewski, K.; Russell, A. J. Synthesis of uniform protein-polymer conjugates. *Biomacromolecules* **2005**, *6* (6), 3380−3387.
(58) Bontempo, D.; Maynard, H. D. Streptavidin as a macroinitiator for polymerization: In situ protein-polymer conjugate formation. *J. Am. Chem. Soc.* **2005**, *127* (18), 6508−6509.
(59) Heredia, K. L.; Bontempo, D.; Ly, T.; Byers, J. T.; Halstenberg, S.; Maynard, H. D. In situ preparation of protein - "Smart" polymer conjugates with retention of bioactivity. *J. Am. Chem. Soc.* **2005**, *127* (48), 16955−16960.
(60) Matyjaszewski, K.; Xia, J. H. Atom transfer radical polymerization. *Chem. Rev.* **2001**, *101* (9), 2921−2990.
(61) Matyjaszewski, K. Atom Transfer Radical Polymerization (ATRP): Current Status and Future Perspectives. *Macromolecules* **2012**, *45* (10), 4015−4039.
(62) Siegwart, D. J.; Oh, J. K.; Matyjaszewski, K. ATRP in the design of functional materials for biomedical applications. *Prog. Polym. Sci.* **2012**, *37* (1), 18−37.
(63) Matyjaszewski, K.; Tsarevsky, N. V. Macromolecular Engineering by Atom Transfer Radical Polymerization. *J. Am. Chem. Soc.* **2014**, *136* (18), 6513−6533.
(64) Zhang, L. B.; Zhao, W. G.; Liu, X. Y.; Wang, G. L.; Wang, Y.; Li, D.; Xie, L. Z.; Gao, Y.; Deng, H. T.; Gao, W. P. Site-selective in situ growth of fluorescent polymer-antibody conjugates with enhanced antigen detection by signal amplification. *Biomaterials* **2015**, *64*, 2−9.
(65) Hu, J.; Wang, G. L.; Zhao, W. G.; Liu, X. Y.; Zhang, L. B.; Gao, W. P. Site-specific in situ growth of an interferon-polymer conjugate that outperforms PEGASYS in cancer therapy. *Biomaterials* **2016**, *96*, 84−92.
(66) Cummings, C. S.; Campbell, A. S.; Baker, S. L.; Carmali, S.; Murata, H.; Russell, A. J. Design of Stomach Acid-Stable and Mucin-Binding Enzyme Polymer Conjugates. *Biomacromolecules* **2017**, *18* (2), 576−586.
(67) Baker, S. L.; Munasinghe, A.; Murata, H.; Lin, P.; Matyjaszewski, K.; Colina, C. M.; Russell, A. J. Intramolecular Interactions of Conjugated Polymers Mimic Molecular Chaperones to Stabilize Protein-Polymer Conjugates. *Biomacromolecules* **2018**, *19* (9), 3798−3813.
(68) Cummings, C. S.; Fein, K.; Murata, H.; Ball, R. L.; Russell, A. J.; Whitehead, K. A. ATRP-grown protein-polymer conjugates containing phenylpiperazine selectively enhance transepithelial protein transport. *J. Controlled Release* **2017**, *255*, 270−278.
(69) Baker, S. L.; Kaupbayeva, B.; Lathwal, S.; Das, S. R.; Russell, A. J.; Matyjaszewski, K. Atom Transfer Radical Polymerization for Biorelated Hybrid Materials. *Biomacromolecules* **2019**, *20* (12), 4272−4298.
(70) Radic, Z.; Dale, T.; Kovarik, Z.; Berend, S.; Garcia, E.; Zhang, L. M.; Amitai, G.; Green, C.; Radic, B.; Duggan, B. M.; Ajami, D.; Rebek, J.; Taylor, P. Catalytic detoxification of nerve agent and pesticide organophosphates by butyrylcholinesterase assisted with non-pyridinium oximes. *Biochem. J.* **2013**, *450*, 231−242.
(71) Zhang, L. B.; Baker, S. L.; Murata, H.; Harris, N.; Ji, W. H.; Amitai, G.; Matyjaszewski, K.; Russell, A. J. Tuning Butyrylcholinesterase Inactivation and Reactivation by Polymer-Based Protein Engineering. *Adv. Sci.* **2020**, *7*, 1901904.
(72) Amitai, G.; Adani, R.; Yacov, G.; Yishay, S.; Teitlboim, S.; Tveria, L.; Limanovich, O.; Kushnir, M.; Meshulam, H. Asymmetric fluorogenic organophosphates for the development of active organophosphate hydrolases with reversed stereoselectivity. *Toxicology* **2007**, *233* (1−3), 187−198.
(73) Murata, H.; Cummings, C. S.; Koepsel, R. R.; Russell, A. J. Polymer-Based Protein Engineering Can Rationally Tune Enzyme Activity, pH-Dependence, and Stability. *Biomacromolecules* **2013**, *14* (6), 1919−1926.
(74) Uttamapinant, C.; Tangpeerachaikul, A.; Grecian, S.; Clarke, S.; Singh, U.; Slade, P.; Gee, K. R.; Ting, A. Y. Fast, Cell-Compatible Click Chemistry with Copper-Chelating Azides for Biomolecular Labeling. *Angew. Chem., Int. Ed.* **2012**, *51* (24), 5852−5856.
(75) Ellman, G. L.; Courtney, K. D.; Andres, V.; Featherstone, R. M. A new and rapid colorimetric determination of acetylcholinesterase activity. *Biochem. Pharmacol.* **1961**, *7* (2), 88−90.
(76) Carmali, S.; Murata, H.; Amemiya, E.; Matyjaszewski, K.; Russell, A. J. Tertiary Structure-Based Prediction of How ATRP Initiators React with Proteins. *ACS Biomater. Sci. Eng.* **2017**, *3*, 2086−2097.
(77) Sumrra, S. H.; Kausar, S.; Raza, M. A.; Zubair, M.; Zafar, M. N.; Nadeem, M. A.; Mughal, E. U.; Chohan, Z. H.; Mushtaq, F.; Rashid, U. Metal based triazole compounds: Their synthesis, computational, antioxidant, enzyme inhibition and antimicrobial properties. *J. Mol. Struct.* **2018**, *1168*, 202−211.
(78) Frasco, M. F.; Fournier, D.; Carvalho, F.; Guilhermino, L. Do metals inhibit acetylcholinesterase (AChE)? Implementation of assay conditions for the use of AChE activity as a biomarker of metal toxicity. *Biomarkers* **2005**, *10* (5), 360−375.
(79) Ribeiro, T. S.; Prates, A.; Alves, S. R.; Oliveira-Silva, J. J.; Riehl, C. A. S.; Figueroa-Villar, J. D. The Effect of Neutral Oximes on the Reactivation of Human Acetylcholinesterase Inhibited with Paraoxon. *J. Braz. Chem. Soc.* **2012**, *23* (7), 1216−1225.
(80) Steinberg, G. M.; Solomon, S. Decomposition of a Phosphonylated Pyridinium Aldoxime in Aqueous Solution. *Biochemistry* **1966**, *5*, 3142−3150.

https://dx.doi.org/10.1021/acs.biomac.0c00959
Biomacromolecules 2020, 21, 3867−3877